Dependence of Core Electronics of Gold Nanoparticles on Ligand, Solvent, and Sample Preparation

Jonathan W. Fagan and Benjamin J. Lear*

Department of Chemistry, The Pennsylvania State University, University Park, PA

E-mail: bul14@psu.edu

Abstract

Electron spin resonance (ESR) spectroscopy is used to probe the electronic properties of the metallic cores of small (ca. 2 nm) gold nanoparticles protected by 1-hexanethiol and 1-dodecanethiol, suspended in either *n*-hexane or THF. Analysis of the ESR spectra allow extraction of the principal components of the *g*-tensor for the metallic electrons in the core. We find that the values associated with the *g*-tensor are sensitive to the identity of both the ligand and the solvent. We also find that the handling of the samples can affect the measured *g*-values, with common manipulations such as freezing and thawing the sample, or precipitating and resuspending the nanoparticles, increasing the measurement-to-measurement distributions in the measured *g*-values. The degree of these perturbations also depends on the identity of the ligand and solvent. These results stress the importance of the design and handling of colloidal systems when seeking to use their electronic behaviors.

Keywords

electron spin resonance, gold nanoparticles, stability, ligand effects, solvent effects

Introduction

Gold nanoparticles are an important component of modern science, used by chemists, materials scientists, physicists, and biologist in order to address a range of fundamental questions regarding the nature of metallic systems[1] and as a platform for cutting-edge applications ranging from lasers[2,3] to sensors[4,5] to cancer treatments.[6,7] The popularity of gold nanoparticles is a result of at least two properties: exciting electronic behaviors that emerge when gold is confined to the nanoscale and the relative robustness of gold particles under typical ambient conditions. For the latter, it is particularly valuable that gold nanoparticles do not experience the oxidation that is common for many other metallic systems, such as copper and silver. However, it is worth acknowledging that this oxidative-centric view of stability is somewhat narrow. Indeed, except for a very few known metallic atomically precise clusters,[8] synthesis of metallic gold nanoparticles results in a heterogeneous population of particles, in terms of size, shape, and surface chemistry—a fact that testifies to a relatively flat energetic landscape for the configuration space. A flat landscape, in turn, implies that gold nanoparticles should be relatively mutable in terms of size, shape, and surface chemistry, post-synthesis.

Importantly, size,[9] shape,[10] and surface chemistry[11–14] are all known to affect the electronic properties of particle's metallic core; the very properties for which the systems are valued. Though they receive less attention in general, effects of surface chemistry are strong enough to affect even the properties of bulk gold.[15] Furthermore, low-barrier restructuring gold surface and absorbates is known to occur for both bulk and nanoscale materials.[16–18] Given the flat configuration landscape for gold nanoparticles, it is reasonable to expect that the structure, and electronic properties, of these particles could be changed during handling of the samples and that even manipulations typically viewed as benign could effect subtle changes in the particle that will manifest as significant changes to the particles electronic properties. These manipulations could even include those routinely employed to *preserve* the particles, such as the freezing (and associated thawing) of samples, and the drying (and

associated resuspension) of colloidal suspensions.

Guided by this line of reasoning, we undertook a study of the electronic properties of small (ca. 2 nm diameter) gold nanoparticles for two different surface chemistries (hexanethiol and dodecanethiol) in two different solvent environments (n-hexane and THF). Below, we will refer to the hexanethiol protected nanoparticles as AuSC6 and the dodecanethiol protected nanoparticles as AuSC12.

The small size of the nanoparticles was chosen to maximize the effect of small changes in structure and surface chemistry. Using these particles, we could determine the effects of changing ligands and solvents on the electronic properties of metallic core. In addition, we wished to determine how stable these properties were. Alkanethiols were chosen because they are commonly employed as stabilizing agents for colloids in non-aqueous media. Both experiment and theory show more favorable absorption energies for longer ligands[19,20] and we were curious if this would translate to particles that were more resistant to perturbation. The solvents were chosen, because THF is known to promote ligand loss,[21] while hexane was expected to be relatively innocent. It was unclear if these differences in solvent would translate to a difference in the degree of perturbation induced by manipulations of the particles. Using pairs of nanoparticles and solvent, we sought to measure how the electronic properties of these systems would change when the samples underwent manipulations common to nanoscience. Specifically, we examined the effects of freezing and thawing the colloidal suspensions and drying and re-constituting the particles (Figure 1).

In order to ascertain changes in the electronic properties of the metallic core, a technique is needed that provides a sensitive and selective measurement of the properties of the metallic core. Though the surface plasmon resonance is often used as a marker for electronic properties of the core, we did not consider using this behavior here, for several reasons. Perhaps most importantly, the plasmon is very strongly damped for the size of the nanoparticles we employed, and it is hard to extract meaningful information from the UV-visible spectrum. An exemplar of the plasmon for our particles can be seen in the SI, which illustrates the

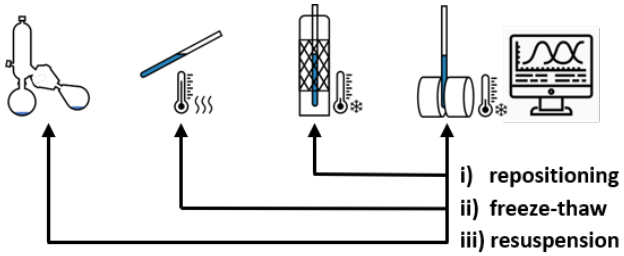

Figure 1: The perturbations to which we exposed our nanoparticles. The first was removal of the frozen sample, and then replacement in the instrument. The second was a thawing of the sample between measurements. The third was removal of the solvent and reconstitution between measurements.

difficulty in analyzing this feature for particles of the size considered herein. However, even if information about the plasmon could be readily extracted, the plasmon resonance is not selective for the electronic structure of the core. For instance, change in the dielectric of the medium surrounding the nanoparticle can produce changes in the plasmon, even if the electronic structure of the metallic core were unaffected. Thus, changes in the plasmon are not a clear indication of changes to the electronic properties of the core. Instead, we turned to electron spin resonance (ESR) to provide a method that would be applicable to particles of our size, and which is are selective for the core properties.

Though metallic gold nanoparticles are often thought of as diamagnetic, paramagnetism can be induced by placing the particles in a magnetic field.[22] This affect is known as Pauli paramagnetism, and results from Zeeman splitting of the band structure, which raises the energy of one electron spin state and lowers the energy of the other. Since metals have partially filled band structures, this will place filled states above empty ones, and electrons will be transferred between spin manifolds, generating a paramagnetism that can be probed via ESR. Importantly, this effect is valid for any metallic system, even for those that have strongly damped plasmons. This makes this approach applicable for our small systems. In addition, because the paramagnetism is a result of the properties of the metallic core, changes in the ESR are directly reporting on changes to the these properties. Perhaps the most direct probe of these electronic properties is the g-value of the unpaired electrons.

Though a detailed discussion of the interpretation of the g-value lies beyond the scope of this report, it is worth noting that its value is connected to both the energy and the nature (e.g., angular momentum) of the electronic state holding the unpaired electron.[22] Thus, changes to the observed g-value indicate changes to the nature of the electronic states within the core. Herein, we use this as a selective probe of metallic properties in order to understand the purturbative nature of common sample manipulations.

Results

We prepared the AuNPs using a modified Brust-Schiffrin method.[23] After synthesis, particles were collected via precipitation and filtration, and then stored as dry powders until the start of the studies, thus, it is worth noting that at least one of the manipulations under consideration occurred prior to the study. More details on the synthesis, sample preparation, and handing can be found in the SI. Particle sizes were determined using TEM. Representative TEM micrographs and the histograms of particle sizes obtained from 200 particle measurements are shown in Figure 2 for particles at the start and end of our studies. In this figure, we also show log-normal fits to these histograms. The mean geometric diameter and geometric standard deviation of the mean obtained from these fits are also given in the figure. More details of the fitting are provided in the SI.

Between the collection of the initial and final TEM images for each particle:solvent pair, we performed 15 EPR measurements. The EPR was collected on a Freiburg Instruments MS-5000X X-band spectrometer with an ER 041MR microwave bridge using a dual-mode ER 4116DM cavity operated in perpendicular TE102 microwave mode with a microwave frequency of 9.623 GHz. Spectra were collected at 25 K in frozen suspensions of either n-hexane or THF. Freezing was performed by slow immersion of an EPR tube containing the AuNP solution into a bath of liquid nitrogen. The sample, approximately 4 cm in height, was immersed into the liquid nitrogen over the course of a minute. The 15 measurements

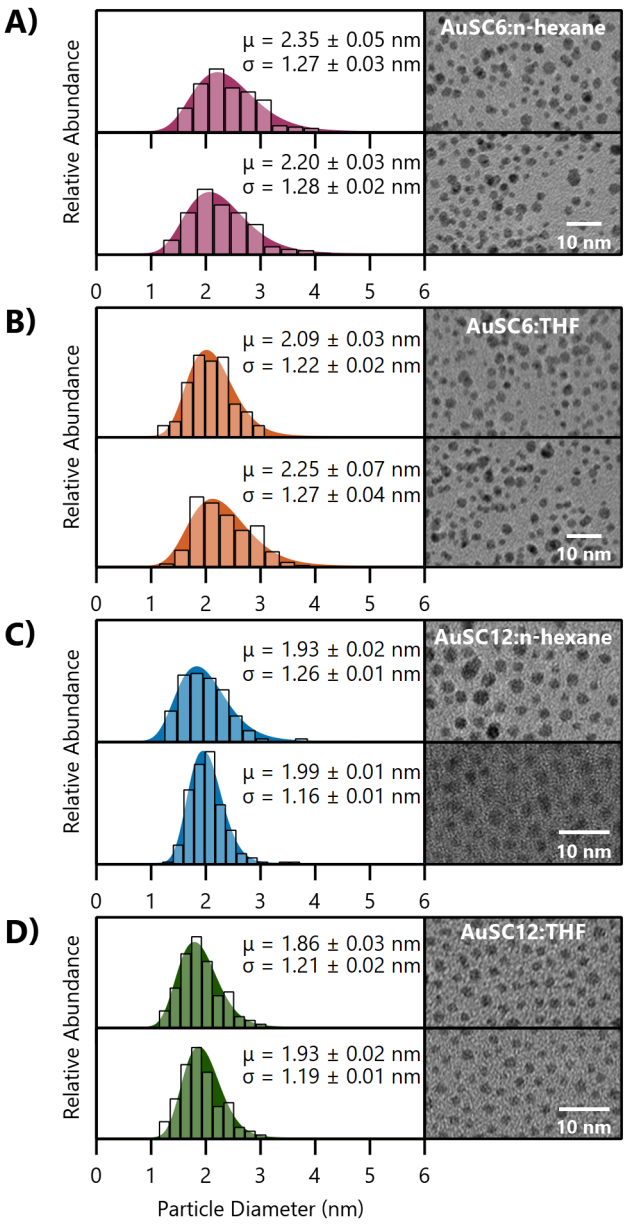

Figure 2: TEM images and histograms of A) AuSC6:*n*-hexane, B) AuSC6:THF, C) AuSC12:*n*-hexane, and D) AuSC12:THF particle diameters obtained from the TEMs, for all four particle:solvent pairs. For each pair, the top image and histogram are of the particles at the start of the manipulations and the bottom image and histogram are of the particles after all 15 manipulations. Also shown are the results of log-normal fits to the histograms, and the geometric mean and geometric standard deviations obtained from these fits, as well as the standard errors in these parameters obtained from the fit.

can be assigned to three sets of 5 measurements each. These sets, shown in Figure 1, can be described, in the order that they were performed, as:

Set 1: Repositioning:

In this set, the EPR tube was removed from the instrument between measurements. The sample remained frozen the entire time. Thus, this condition probes the perturbation associated with sample position within the EPR resonance cavity. Because this is not expected to produce a change in the sample, this set provides a baseline for the variation in spectra collection, to which we can compare the following two sets.

Set 2: Freeze-thaw:

In this set, the EPR tube was removed from the instrument and allowed to thaw between measurements. The sample was then frozen and re-inserted into the resonance cavity to collect the new spectra. As above, freezing was performed by slow immersion of an EPR tube containing the AuNP solution into a bath of liquid nitrogen. Thus, this set probes the perturbation induced simply from moving between liquid and solid states of the sample. Often times, samples are preserved by freezing them. While this is often effective for atomically precise samples that are relatively stable, it is unclear how effective this method would be for heterogeneous nanoscale materials that reside on a much flatter energetic landscape.

Set 3: Resuspension

In this set, the sample was thawed and the solvent removed by rotary evaporation between measurements. The sample was then resuspended before being frozen and the next spectra acquired. As for the first two sets, freezing was performed by slow immersion of the sample in a liquid nitrogen bath. The removal of solvent to store samples as powders is also common practice in nanoscience. However, the process of solvent removal is likely more perturbative than simple freezing of samples, and this set tests that hypothesis with respect to the electronic properties of the metallic core.

In total, across the four nanoparticle:solvent pairs, we collected 60 different EPR spectra

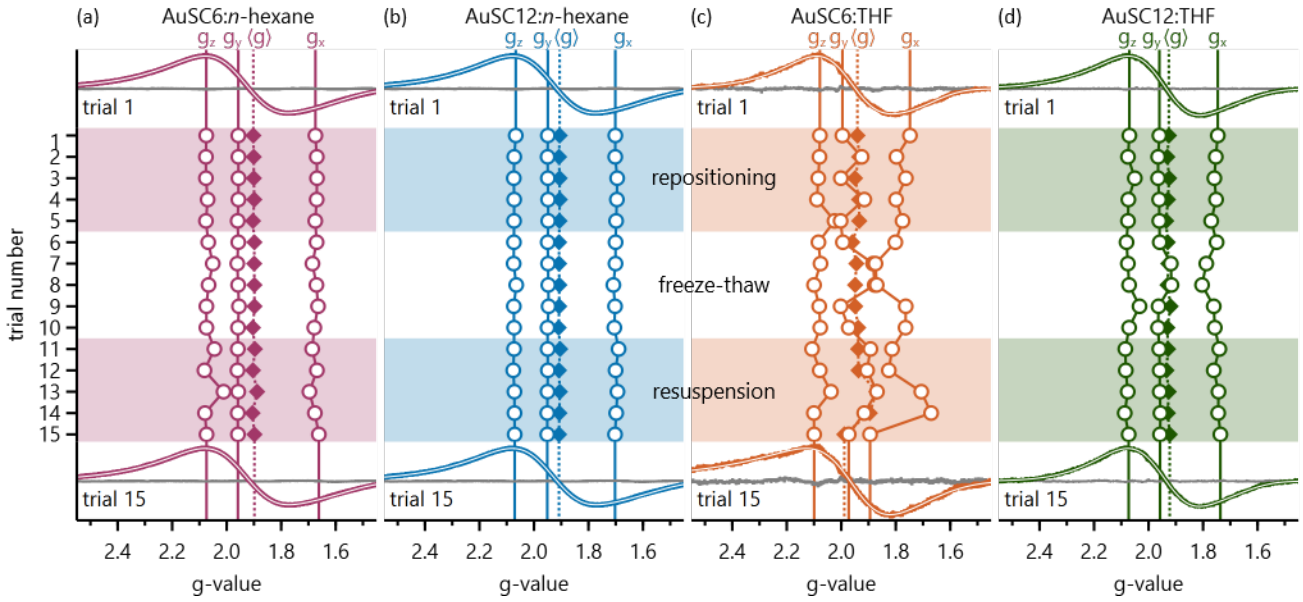

Figure 3: ESR spectra and extracted g-values for all samples, grouped by nanoparticle:solvent pair. For each, the starting ESR spectra are at the top and the final ESR spectra are at the bottom. For these spectra, the experimental data is the colored line, the fit is the white line, and the residuals are the grey line. Also indicated are the position of g_x, g_y, g_z, and $\langle g \rangle$, extracted from the fit. Between the two spectra are shown the values for these parameters for each trial. The shaded regions indicate the nature of the trial, for three different perturbations performed between measurements: repositioning of the ESR tube, thawing and re-freezing of the EPR tube, and drying and re suspension of the nanoparticles. For clarity, the standard errors of these parameters are not shown, though they can be found in Table S1 and seen in Figure 4 for $\langle g \rangle$ and the SI for the remaining parameters.

and fit them to an EPR powder pattern built from individual Gaussian band shapes, using a home-built Python program described in detail elsewhere.[24] Each spectrum and its fit can be seen in the SI. Figure 3 shows the initial and final spectra for each nanoparticle:solvent pair. These are the spectra most closely associated with the TEM distributions shown in Figure 2. In Figure 3, the experimental spectra are shown as the colored line, the fit as the white line, and the residual of the fit as the grey line. Fitting of the spectra allows extraction of the g-value. Because we are working with frozen solutions, the tensor nature of the g-value is manifest in the line shape and we extract positions for the three principal components, g_x, g_y, and g_z, shown as the vertical lines in Figure 3. Using these principal components, we can calculate the value of the isotropic g-value, $\langle g \rangle$, which is given by the arithmetic mean of the principal values and is the value expected for a rotationally averaged spectra (i.e., in liquid state). We note that we used frozen colloidal suspensions in our experiments, because the ESR spectra becomes too lifetime broadened to observe at temperatures where either hexane or THF are liquid. However, $\langle g \rangle$ is a value that will have relevance for researchers employing nanoparticle suspensions in the liquid state, and so we also report it here. The $\langle g \rangle$ value are shown in Figure 3 using vertical dashed lines.

Between the first and last spectra in Figure 3, we show the evolution of g_x, g_y, g_z, and $\langle g \rangle$ values for each measurement. All of these values, and the errors associated with them, are given in Tables S1-S4. Our fits also yields values of the widths associated with the principal g-tensor values, and these are also presented in Tables S1-S4. Here, we focus on the values associated with the g-tensor, rather than the widths, as they are more directly connected to the electronic structure of the nanoparticle.

Discussion

Examination of Figure 3 reveals several trends in the parameters extracted from the ESR spectra. First, it is clear that, for all samples, the values of $\langle g \rangle$ experience less fluctuation

than the individual principal components of the g-tensor. In other words, changes in the different g-tensor values tend to offset one another. This makes sense if one assumes that changes to the g-tensor reflect restructuring of the particles. The standard explanation for different values of g_x, g_y, and g_z in molecules that they reflect asymmetries in in the structure of the molecule. We have recently suggested that a similar interpretation should be used for nanoparticles.[24] This implies that the values of g_x, g_y, and g_z are tied to physical morphology of the particle. Because there is a fixed amount of gold and ligand in the sample, a change along one dimension of the particle will invoke a change along another. For instance, growth along the particle z-axis will come at the expense of material along either the x- or y-axes—or both. While it is important to note that the particle's geometric axes need not correspond directly to the g-tensor axes, a similar logic will follow if the alignment between the g-tensor and molecular geometry was known. This line of reasoning suggests a rational for why the changes in g_x, g_y, and g_z tend to offset. If this hypothesis is true, then the value of $g_z - g_x$ could function as a measure of a sort of aspect ratio of the particle, though more work is needed to firmly establish such a quantitative relationship. Of course, there does not need to be a linear relationship between morphological changes, and this could account for why there is still some change in the observed $\langle g \rangle$, as the g_x, g_y, and g_z change.

Though these changes are cast in terms of changes to the morphology of the core atoms, it is worth acknowledging that ligands and solvent play a role. In particular, it is expected that the solvent interaction with the ligands helps to facilitate re-arrangements of the ligands and, through the strong bonds to the gold, the gold atoms of the core. Thus, we believe that both the core atoms and the ligand structure is changing. However, as ESR probes the metallic electrons, which should be localized on the core over the ligands, our measurements are anticipated to be more sensitive to the properties of the core, and so we frame our interpretation with respect to the core.

Another feature that stands out is that the values present for the particles in n-hexane (Figure 3a,b) experience less fluctuation than for the same particles in THF (Figure 3c,d).

In addition, we also find that for a particular solvent, the AuSC6 particles (Figure 3a,c) have more variation in their g-values than the AuSC12 particles (Figure 3b,d). To make these behaviors easier to see, Figure 4 shows just the $\langle g \rangle$ values for all four nanoparticle:solvent pairs. Also shown are the errors associated with the fit. In this figure, the shaded regions represent the 90% confidence intervals for the collection of 5 measurements for each set. Analogous figures for the g_x, g_y, and g_z values, as well as G_x, G_y, and G_z are given in the SI.

From Figure 4, it is immediately clear that, when comparing changes in solvent alone, the distributions in n-hexane are more narrow than in THF. Similarly, when comparing changes in ligand alone, distributions for particle protected in dodecanethiol are more narrow than for particles protected by hexanethiol. Again, if one is attempting to preserve electronic properties, our results suggest that long-chain ligands are to be preferred, as are non-polar solvents.

Another feature that becomes clear from examination of Figure 4 is that the first and second sets of conditions (repositioning and freeze-thaw) are equally pertabative. On the other hand, the condition under which we remove solvent and then resuspend particles between measurements is more purturbative, especially for the AuSC6 particles. It is worth noting, that, using an f-test, the change in the spread of values as one moves through the manipulations for a particular solvent:solvent pair is only significant at the 95% confidence limit for the AuSC6 particles. Nevertheless, if one wishes to preserve the electronic properties of nanoparticles, it seems that freezing is to be preferred to drying.

It is worth noting that, especially for the AuSC6:THF sample the individual spectra (Figure S3) are clearly noisier than for the other nanoparticle:solvent pairs, and this noise will introduce additional uncertainties and fluctuations in the the extracted parameters. However, the increased uncertainty in the parameter values is unlikely to explain the entire increase in the distribution of values, especially those seen when the particles undergo drying and re-suspension. Thus, the uncertainty due to increased spectra noise is unlikely to explain

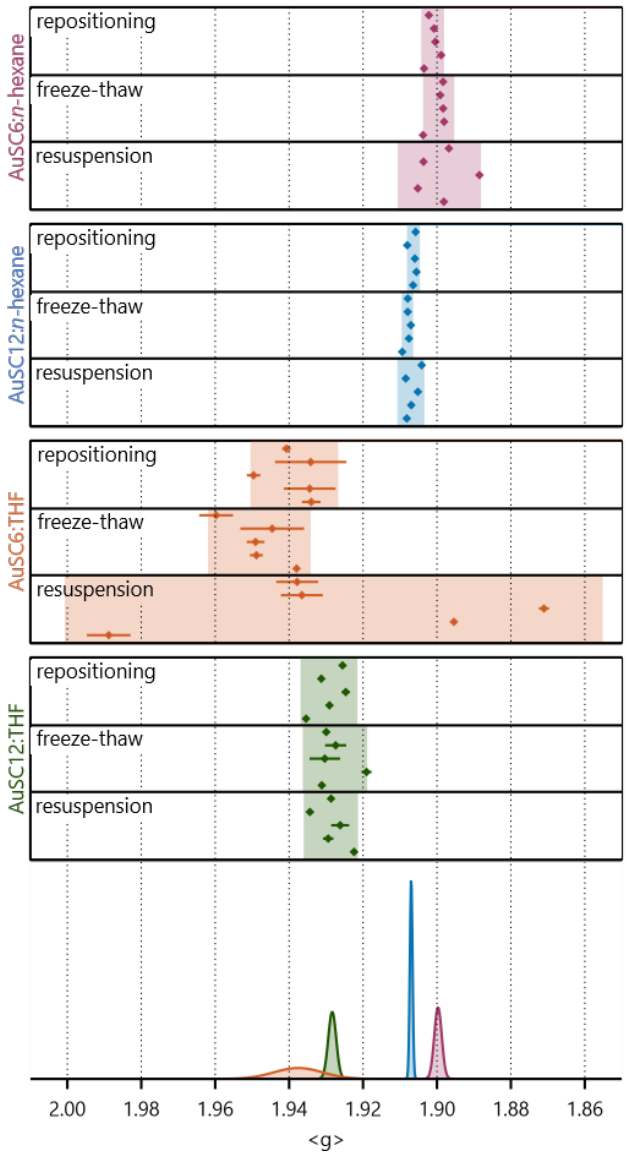

Figure 4: Collected values of $\langle g \rangle$ for all samples. The individual points and bars indicate the mean value and standard error from the fit. The shaded regions indicate the 90% confidence intervals associated with each grouping of 5 measurements. The bottom figure gives the Gaussian distributions associated with the mean value of all 15 measurements for each sample, and the width of the distribution is given by the standard error of this mean.

all of the increased fluctuation the extracted values of the parameters.

Interestingly, though the distribution of values does change between sets of measurements, the mean value for a particular particle:solvent pair does not. If we use a t-test to compare the values for all of the g-tensor components, the $\langle g \rangle$, and the FWHM values, we find that *none* of these parameters experience a change in their mean values, within a 95% confidence limit. This is true in two ways.

First, we can compare the first and final measurements. These are the measurements for which we have TEM images. For this we assume an error in a single measurement defined by the value for the first 5 measurements, as this standard error is larger than that estimated from the fit. Doing so, we find that *none* of the final values vary significantly from the initial values, according to the results of a t-test at the 95% confidence limit.

The second way in which we can see that values do not change is to compare the means of the first, second, and third sets of measurements, using the standard deviations of each set to provide a standard error for the mean value. Doing so, we again find that *none* of the means are significantly different, again using a t-test at the 95% confidence limit. In other words, though the values do fluctuate more when the samples undergo resuspension from the solid state, they continue to fluctuate about the mean value attained in the first set of measurements. This also suggests that the perturbations associated with sample drying are more of a concern if one is considering individual usages of the particles, rather than an average across multiple usages. This highlights the need to consider the use case of nanoparticles, when choosing how to store and manipulate them.

The result that all measurements for each nanoparticle:solvent pair fluctuate about a common mean is important for this study, as it allows us to group all 15 measurements for a nanoparticle:solvent pair together and calculate the common mean value and standard error associated with this mean. Gaussian distributions plotted using these values are shown on the bottom of Figure 4 for $\langle g \rangle$. From the values in Figure 4, we find the following to be true:

1. A change in ligand produces a statistically significant change in $\langle g \rangle$ at 95% confidence

using a t-test. In other words, we again see that changes as subtle as ligand length produce significant differences in the electronic properties of the metallic *core*.

2. For the ligands studied here, a change in solvent from hexane to THF, produces a larger shift in $\langle g \rangle$ than a change in ligand. In other words, changes in the solvent can produce changes in the electronic properties of the metallic *core*.

3. The distribution of values for $\langle g \rangle$ is significantly (95% confidence, using an f-test) narrower for AuSC12 than AuSC6, when in the same solvents. In other words, AuSC12 produce particles with more stable properties of the metallic *core*.

4. The distribution of values for $\langle g \rangle$ is significantly (95% confidence, using an f-test) narrower for both particles in hexane, as compared to THF. In other words, the electronic properties of the metallic *core* are more stable in hexane than THF.

5. The change in the width of the distributions $\langle g \rangle$ between AuSC12 in THF versus hexane is roughly the same as between AuSC12 and AuCS6 in THF or hexane.

Similar trends are found for the principal components of the g-tensor, as shown in the SI. In other words, the ligand and solvent provide similar power in controlling the stability of the electronic properties of the metallic *core*. This is a testament to the ability of the ligand and solvent to mediate and promote changes to the core structure which, as noted above, is primarily were the electrons we probe are localized.

Conclusions

Using electron spin resonance, we demonstrate the nature of environmental control over the electronic properties of the *core* of metallic nanoparticles. In particular, we have shown that the electronic properties of nanoparticles respond to even subtle changes in environment, such as changing the ligand length from hexanethiol to dodecanethiol while in n-hexane. These

results also suggests that, while guidance can be given in how to best preserve nanoparticles, it may be that the best choice of ligand and solvent with regard to stability are not the best in terms of electronic properties. It remains up to the researcher to balance the relative importance of these behaviors. However, our results here demonstrate that both environmental and ligand parameters are important, when seeking to leverage the behaviors of mutable nanoparticle systems.

Acknowledgement

The authors thank the NSF (CHE-1362825) for financial support of this work.

Supporting Information Available

Synthetic route, fitting procedures for the ESR, tables and plots of parameters extracted from the fitting.

References

(1) Halperin, W. P. Quantum Size Effects in Metal Particles. *Review of Modern Physics* **1986**, *58*, 533–606.

(2) Oulton, R. F.; Orger, V. J.; Zentgraf, T.; Ma, R. M.; Gladden, C.; Dai, L.; Bartal, G.; Zhang, X. Plasmonic lasers at deep subwavelength scale. *Nature* **2009**, *461*, 629–632.

(3) Sidiropoulos, T. P. . H.; Roder, R.; Geburt, S.; Hess, O.; Maier, S. A.; Ronning, C.; Oulton, R. F. Ultrafast plasmonic nanowire lasers near the surface plasmon frequency. *Nature Physics* **2014**, *10*, 870–876.

(4) Stawart, M. E.; Anderton, C. R.; Thompson, L. B.; Maria, J.; Gray, A. K.; Rogers, J. A.;

Nuzzo, R. G. Nanostructured Plasmonic Sensors. *Chemical Reviews* **2008**, *108*, 494–521.

(5) Willets, K. A.; Duyne, R. P. V. Localized Surface Plasmon Resonance Spectroscopy and Sensing. *Annual Review of Physical Chemistry* **2007**, *58*, 267–297.

(6) Dreaden, E. C.; Alkilany, A. M.; Huang, X.; Murphy, C. J.; El-Sayed, M. A. The golden age: gold nanoparticles for biomedicine. *Chemical Society Reviews* **2012**, *41*, 2740–2279.

(7) Bardhan, I.; Lal, S.; Joshi, A.; Halas, N. J. Theranostic Nanoschells: From Probe Design to Imaging and Treatment of Cancer. *Accounts of Chemical Research* **2011**, *44*, 936–946.

(8) Jin, R.; Zeng, C.; Zhou, M.; Chen, Y. Atomically Precise Colloidal Metal Nanoclusters and Nanoparticles: Fundamentals and Opportunities. *Chemical Reviews* **2016**, *116*, 10346–10413, PMID: 27585252.

(9) Link, S.; El-Sayed, M. Size and Temperature Dependence of the Plasmon Absorption of Colloidal Gold Nanoparticles. *The Journal of Physical Chemistry B* **1999**, *103*, 4212–4217.

(10) Chen, H.; Kou, X.; Yang, Z.; Ni, W.; Wang, J. Shape- and Size-Dependent Refractive Index Sensitivity of Gold Nanoparticles. *Langmuir* **2008**, *24*, 5233–5237.

(11) Cirri, A.; Silakov, A.; Jensen, L.; Lear, B. J. Chain Length and Solvent Control over the Electronic Properties of Alkanethiolate-Protected Gold Nanoparticles at the Molecule-to-Metal Transition. *Journal of the American Chemical Society* **2016**, *138*, 15987–15993, PMID: 27960314.

(12) Gosh, S. K.; Nath, S.; Kundu, S.; Esumi, K.; Pal, T. Solvent and Ligand effects on

the Localized Surface Plasmon Resonance (LSPR) of Gold Colloids. *The Journal of Physical Chemistry B* **2004**, *108*, 13963–13971.

(13) Andolina, C. M.; Dewar, A. C.; Smith, A. M.; Marbella, L. E.; Hartmann, M. J.; Millstone, J. E. Photoluminescent Gold–Copper Nanoparticle Alloys with Composition-Tunable Near-Infrared Emission. *Journal of the American Chemical Society* **2013**, *135*, 5266–5269.

(14) Aruda, K. O.; Tagliazucchi, M.; Sweeney, C. M.; Hannah, D. C.; Weiss, E. A. The role of interfacial charge transfer-type interactions in the decay of plasmon excitations in metal nanoparticles. *Phys. Chem. Chem. Phys.* **2013**, *15*, 7441–7449.

(15) Evans, S. D.; Ulman, A. Surface potential studies of alkyl-thiol monolayers adsorbed on gold. *Chemical Physics Letters* **1990**, *170*, 462–466.

(16) Suzuki, Y.; Kizuka, T. Surface reconstruction in gold nanowires. *Scientific Reports* **2018**, 9836.

(17) Liu1, P.; Madsen, J.; Schiøtz, J.; Wagner, J. B.; Hansen, T. W. Reversible and concerted atom diffusion on supported gold nanoparticles. *J. Phys. Mat.* **2020**, 024009.

(18) Doña, J.; González-Velasco, J. The dependence of the surface diffusion coefficients of gold atoms on the potential: its influence on reconstruction of metal lattices. *Surface Science* **1992**, *274*, 205 – 214.

(19) Yuan, Y.; Yam, C.; Shmakova, O.; Colorado, R.; Graupe, M.; Fukushima, H.; Moore, H.; Lee, T. Solution-Phase Desorption of Self-Assembled Monolayers on Gold Derived From Terminally Perfluorinated Alkanethiols. *The Journal of Physical Chemistry C* **2011**, *115*, 19749–19760.

(20) Mete, E.; Yortanlı, M.; Danışman, M. F. A van der Waals DFT study of chain length

dependence of alkanethiol adsorption on Au(111): physisorption vs. chemisorption. *Phys. Chem. Chem. Phys.* **2017**, *19*, 13756–13766.

(21) Huang, Y.; Liu, W.; Cheng, H.; Yao, T.; Yang, L.; Bao, J.; Huang, T.; Sun, Z.; Jiang, Y.; Wei, S. Solvent-induced desorption of alkanethiol ligands from Au nanoparticles. *Phys. Chem. Chem. Phys.* **2016**, *18*, 15927–15933.

(22) Blundell, S. *Magnetism in Condensed Matter*; Oxford University Press: Oxford, UK, 2001.

(23) Brust, M.; Walker, M.; Bethell, D.; Schiffrin, D. J.; Whyman, R. Synthesis of thiol-derivatised gold nanoparticles in a two-phase Liquid–Liquid system. *J. Chem. Soc., Chem. Commun.* **1994**, 801–802.

(24) Cruz, S.; Tanygin, V.; Lear, B. J. Effect of asymmetry on EPR. *ACS Nano* **Submitted**,

Graphical TOC Entry